

Design and Development of a Monolithic Gripper with Flexural Joints for Macroscale Manipulation

Ngonidzaishe N. Mrewa, Ahmed M. R. Fath Elbab and George N. Nyakoe

Abstract—This paper presents a robotic gripper design which enacts flexural joints rather than prismatic and revolute joints to ensure gripping action. The designed flexure-based gripper exhibits large displacement than is normally possible with such joint-types in effect. With large displacements, the gripper used to handle kiwifruit and at the same time determine its softness. Flexural joint mechanism is based on the intrinsic compliancy of a material to achieve structural elastic deformation and execute the requisite displacement. The monolithic model is designed to demand more lumped compliancy displacement than distributed compliancy. The feasibility of the design is examined through a series of numerical analysis and simulations on COMSOL platform leading to subtractive fabrication of the prototype.

Keywords—flexure joints, large displacement, lumped compliancy, monolithic.

I. INTRODUCTION

THE most common type of grippers are mechanical grippers, vacuum grippers, pneumatic grippers, hydraulic grippers and magnetic grippers[1][2]. Newer technologies involve the use of soft grippers from highly compliant materials such as silicone, rubber and other elastomeric polymers[3]. The use of flexural joints mechanism is highly prevalent in Micro Electromechanical Systems (MEMS) technology. Implementation of flexural joints in conventional robotic gripping has not been conceived because of the small displacements associated with flexure joints[4][6]. Notwithstanding, the development of a monolithic structure becomes possible with the use of flexural joint mechanism. The major reason for the developing the gripper as a monolithic structure is because it accommodates any possible future intergration with microelectronics. In addition, a monolithic structure eradicates the need for assembly to construct the gripper and consequently relative reduction in fabrication costs[7]. Furthermore, any friction related ramifications like backlash, wear and loss of accuracy are not a factor. With flexure joints being either producing lumped or distributed compliancy[8], various lumped flexure joints have been developed, and a study to compare the performances of one against another[7][9][10]. As presented in [7], flexure hinges of rectangular, circular and parabolic form were evaluated against each other to determine which one has the edge above the others in terms of maximizing deformation from applied forces, stiffness profile along the joints and

the stress analysis. Other authors have transformed already existing prismatic and revolute joints into their flexure joints counterparts [4] using the rigid-compliant mechanism transformation process. The pseudo-rigid-body model is employed as a license to apply similar kinematic analysis procedures as the ones used for traditional rigid joints. Many designs have been introduced, customized for the very purposes for which they were developed[11][13][9], with [13] producing an atlas of most flexure-based grippers already designed. The closest to achieving macroscale gripping with flexure joints was [14], obtaining a maximum of 0.14mm from circular flexure joints. Most flexure based grippers are normally open grippers. Therefore, their fingers are designed with a gap that is slightly larger than the object to be manipulated[5]. The extra space is within the gripping stroke of both fingers. The development of this flexure-based gripper had to undergo three areas of design criteria scrutiny: materials analysis, structural analysis and optimization of the geometry and thirdly the boundary and loading conditions the gripper is exposed to[7]. Material analysis handles the stiffness analysis, modulus of elasticity, material weight, availability and cost. Plexiglas was used for the purposes of this research. The datasheet is provided in [15]. Structural analysis involves critical detailing of all dimensions and sections of the gripper. This also involves the gripping mechanism employed and the expected motion of the fingers[16] so as to realize maximum deformation from the joints without overdesigning or drastically reducing the number of cycles. The gripper has been designed to carry out friction type gripping mechanism during manipulation since the fingers are rectangular in shape. To obtain translational motion from the fingers, the parallelogram 4-bar mechanism concept has been adopted[9][17][20]. The 4-bar linkage ensures that displacement occurs only in one direction for the planar gripper, thereby eliminating any rotary approach to the object of manipulation. Lumped-type circular joints are planted on the 4-bar linkage. The macroscale gripper has a range falling in the millimeter scale. Therefore, it was designed to manipulate kiwifruit without causing any harm to the fruits. Other medium-sized fruits or objects with weight and dimensional properties similar to those of kiwifruit can be manipulated with the same gripper. For larger or smaller fruits, the design will have to be customized for the same. Following 3D CAD design which is proven by analytical simulation, a numerical simulation was conducted using ANSYS and COMSOL software platforms to verify the viability of the design. A monolithic prototype was fabricated using laser machining. Hence, this paper discusses the design criteria implemented in order to realize the gripper model, the executed

Ngonidzaishe N. Mrewa, Department of Mechatronics Engineering, PAUSTI (+254746266043; e-mail: nmrewa@yahoo.com).

Ahmed M. R. Fath Elbab, Department of Mechatronics and Robotics, E-JUST (e-mail: ahmed.rashad@ejust.edu.eg).

George N. Nyakoe, Department of Electrical Engineering, JKUAT (e-mail: nyakoe@eng.jkuat.ac.ke).

TABLE I
PHYSICAL PROPERTIES OF COMMON ENGINEERING MATERIALS

| Material | Strength (MPa) | Young's Modulus (GPa) | Resilience | Material Density (kg/m ³) |
|-----------|----------------|-----------------------|------------|---------------------------------------|
| Plexiglas | 69 | 2.8 | 0.025 | 1119 |
| Steel | 1641 | 207 | 0.0079 | 8050 |
| Aluminum | 503 | 71.7 | 0.007 | 2700 |
| E-glass | 1640 | 56 | 0.029 | 1900 |

FEA computation and the fabrication and performance of the gripper prototype.

II. MECHANICAL GRIPPER DESIGN

A. Materials analysis

In determining the material to be used, an arbitrary criterion with different weight factor was considered. The properties involved include material properties, cost and availability.

1) *Material properties:* A material to be used for flexural joint implementation ought to display a high acceptance to any deflection related motion and high resistance to failure, fracture or loss of elasticity. To achieve this, a highly flexible and strong material is required. The flexibility of any material is largely dependent on its Youngs modulus[7]. Therefore, the ratio of the two parameters, termed the modulus of resilience, and the material weight are the material properties considered. Plexiglas has a resilience which is higher than most engineering materials given in Table 1. It has the lowest density value amongst the materials.

2) *Cost:* The idea behind cost determination focuses on the cost of the material itself and the cost related to its fabrication process. Low cost material and production makes mass production of monolithic grippers possible without lag time affecting the process.

3) *Availability:* Materials readily available in the market makes it easy for the industry to reproduce the gripper. Plexiglas is a common material available both in the local, global and online market.

B. Geometrical Analysis

Every aspect of the gripper had to be specially designed in order to achieve large output displacements, low element stresses, small driving forces, high mechanical advantage or displacement amplification factor and low power consumption. Nonetheless, trade-offs were made for other criterion so as to maintain the strength of other implemented measures.

1) *Fingers/tips:* The length of the fingers was arrived at with the object of manipulation in consideration. A short length of 40mm was given to the fingers to avert high finger deformation leading to corresponding reduction in grasp firmness. The gripper is a normally open gripper. The distance separating the two fingers depends upon the object of manipulation and the gripping stroke of each finger. A distance of 52mm exists between the two fingers when they are in repose. The parallel orientation of the gripper portrays

the translational movement expected of the gripper. The fingers are rectangular shaped, with the same thickness as that of the whole gripper. Therefore, the grasped object is solely clenched by friction retention during manipulation.

2) *Actuator bracket:* The bracket is developed for input force transfer to the gripper. It is an interface between the actuator and the gripper itself. Its connections does not constrain any movement of the grippers active elements. It is fashioned to match the type of actuator used. A miniature linear motion actuator from Firgelli is used, having a 50mm stroke and 256:1 gear ratio.

3) *Gripper active elements:* The angle of inclination which the active elements make with the transverse axis of the gripper is essential to increase the displacement amplification. When the angle of inclination from the transverse axis is small, more planar motion of the fingers towards each other is achieved. This is because the x-component of the applied force, $F\cos\theta$, is at an elevated margin when angle θ is small. In this case, the elements are inclined at a 45° angle.

4) *Flexure joints:* Flexure joints either produce lumped or distributed compliancy. This can be depicted in Fig 1. The monolithic gripper exploits on lumped compliancy more than distributed compliancy in the ploy to achieve maximum deformation in the material structure. The choice of notch type selected was based on the attainable motion range and associated stress concentration, the compactness of the joint, robustness and the off-axis stiffness[21]. Circular notch type hinges were adopted its characteristics were most suitable in this situation. The stiffness equation was adopted from [22]. The variables for the dimensions can be determined from Fig 2.

$$K_b = \frac{2Ebt^{\frac{5}{2}}}{9\pi r^{\frac{1}{2}}} \quad (1)$$

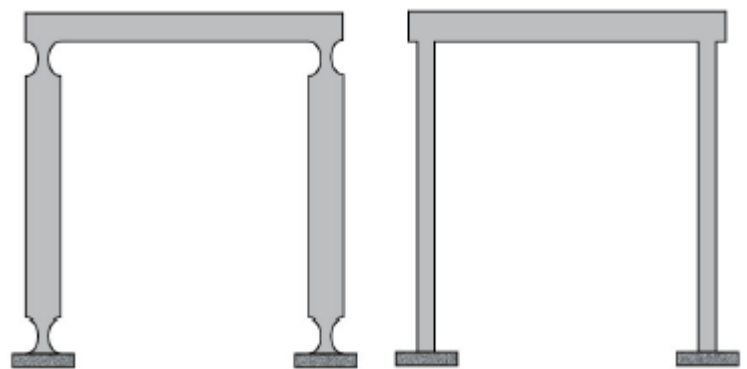


Fig. 1. (a) lumped compliance

(b) distributed compliance[8]

Hence, each joint has a stiffness of 6.3 N/m. The maximum allowable elastic deformation and the stiffness with its corresponding stress were major determinants when arriving at the optimum joint thickness befitting this design. Subjecting only one joint to stresses required to attain the desired displacement

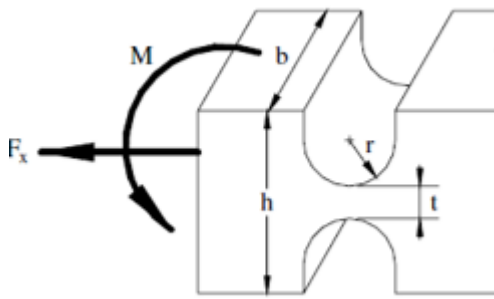


Fig. 2. Variable assignment of joint dimensions[22]

would be irrational. Hence, generating multiple active flexure joints along the gripper links would result in stress and deformation distribution amongst the joints. The distribution profile, however, is somehow unevenly arrayed and it depends on the number of joints used, separation distance, and the type of joint. This design employed 8 active joints for the inner links and 9 for the outer links.

5) *Gripper links*: The length, angle and nature of the links are fundamental features to promote huge deformations. As a way to ensure the translational motion of the gripper fingers and hence strategic dexterity of grasping action, a parallelogram mechanism using a 4 bar linkage was used. The mechanism enhances planar motion in one direction, thereby inhibiting any imminent toggle movement. The links are populated with multiple active flexure joints to further maximize displacement. The stiffness of a structure and the moment encountered is directly associated with the length of the member. This is based on equation 2 and 3.

$$K = \frac{EA}{L} \quad (2)$$

$$Moment = FL \quad (3)$$

The longer the link, the lesser the stiffness translating to more deformation. The moment is directly proportional to length L , which translates to more deformation as well. Links of 112mm vertical dimensions are used. Each set of links forming a parallelogram was brought closer together to increase both stiffness and deflection. Because the links are so close together, they operate almost as a single thick layer hence making it stiffer. The more the parallelogram links are apart, the more the force is directed only towards one link, making the other link ineffective and a displacement impedes to the active link. The links are separated by a distance of 5mm.

The angle of inclination that the links make with the transverse axis and also the active elements affects the force transfer to the fingers. The links incline at an angle of 65° to the transverse axis and 69° inner angle to the active elements. Maximizing the capitalization of these angles was impeded by the set distance between the fingers and the size and shape optimization of the overall gripper.

6) *Gripper base*: The base must be strong enough to support the attached links and the actuator. A customized actuator provision is allotted on the base profile. The wing-sides of the base are cutoff as a topology optimization implementation.

7) *Type of actuator*: The actuator used was chosen based on the level of control to be implemented, the cost, and the anticipated input and output displacement. With the need for precision gripping and force control in order to ensure meticulous fruit gripping without affecting the integrity of the fruit by damaging it, as well as softness determination of the fruit, an electric linear actuator is used[23]. The actuator has a 50mm stroke and a gear ratio of 256:1. The mode of operation is either through a computer or through pulse width module. All these modes require a power source of 3.3V for the operation of the actuator. Other specifications of interest for selection were size, step size, repeatability, speed and range of force.

8) *Force sensing and control*: The force sensor is used to make the gripper smart by becoming capable of determining the force being applied and consequently the softness of the fruit. This simplifies the sorting process. The force sensor is aligned along the profile of the fingers, being placed on an 18mm cylindrical disc. The cylindrical discs can be seen in Fig 2. Force-sensitive resistors (FSR) will be used. Their resistance change in proportion to the amount of pressure applied. They are of low cost and measure forces ranging from 0-100N, which is within the operating range of the fruit gripping. A combination of the linear actuator control board and Arduino microcontroller are used for force and positioning control. From the applied force between the fingers and the fruit, the resistance of the FSR decreases. The resistance is changed into voltage for the purpose of producing an analog input to the controller. This feedback signal determines whether the actuator should stop, actuate more or retract.

C. Boundary and loading conditions

All rotational motion has been inhibited. The fingers can only operate in one plane. The orientation of approach of the gripper to the object of manipulation is threefold: Vertical Gripper - Horizontal Fruit

Vertical Gripper - Vertical Fruit

Horizontal Gripper - Vertical Fruit

The base is stationary and the links and the active elements are dynamic. The actuating force is exerted on the active elements through the actuating point, which then transmit the force to the links and eventually the fingers. The retraction motion of the actuator causes a closure of the gripper fingers, thereby gripping the fruit. Actuation causes the gripper to relax its grasp on the fruit and hence dropping the fruit after manipulation. The force on the fruit is enough to prevent slippage and fruit damage simultaneously. A slight load due to the weight of the fruit is experienced inside the inner profile of the fingers, and is accounted for during simulations.

III. KINEMATIC ANALYSIS

To analyze the kinematics of the gripper, the Pseudo-Rigid-Body Model (PRBM) is implemented[8], [10], [13]. The dynamic and kinematic analysis for force determination were adopted from [24]. The analysis involving displacement considerations and stress evaluation were adopted from [14], [25].

The model assists in determining the grasping force necessary to hold the object (fruits) in place during manipulation.

$$F = K_1 K_2 K_3 \times mg \quad (4)$$

F is gripping force

K_1 is factor of safety (ranges from 1.2 - 2.0)

K_2 is $1+ A/g$ (A is acceleration during manipulation)

K_3 is transfer coefficient of gripper

Therefore, for this fruit gripper, the tensile strength of the gripper is 69MPa, and the allowable applied stress shall be 46MPa, hence giving a factor of safety of 1.5. The least possible F.o.S has been chosen because Plexiglas is not a compliant material. So allowing for the highest possible flexibility will ensure more displacement. A maximum acceleration of $0.04m/s^2$ is used. (4g maximum acceleration).

$$K_2 = 1 + (0.04/9.81) = 1.0041 \quad (5)$$

The transfer coefficient for the gripper orientation of;

1. Horizontal gripper, vertical object

2. Vertical gripper, vertical object

These orientations demand a transfer coefficient of $1/2\mu$ [24].

Making use of the Amonton-Coulomb friction model, having the following parameters;

Maximum weight of kiwifruit is 0.075kg[26].

$$F_g = 0.075kg \times 9.81m/s^2 = 0.736N \quad (6)$$

= friction coefficient

$$K_3 = \frac{1}{(2 \times 0.4)} = \frac{1}{0.8} = 1.25 \quad (7)$$

Therefore, the necessary grasping force during manipulation is given by;

$$F = 1.5 \times 1.0041 \times 1.23 \times 0.736 = 1.4N \quad (8)$$

The geometry of the gripper can be likened the one given in Fig 3 save for the fact that it uses rigid joints instead of flexure joints. The gripper with rigid joints in Fig 3 is an extract from [24]; Due to the geometric construction of the gripper, the relationship between actuator force and gripping force is given by;

$$P = \frac{2FL\cos\theta}{R} \quad (9)$$

$$P = \frac{1.4 \times 2 \times 0.123578 \times \cos 25^\circ}{0.05565} = 6.0N \quad (10)$$

Only the length (L) of the links has direct positive correlation with the actuating force. The half-length of the base (R) and the angle of inclination (θ) both provide negative interdependence. The linear contribution of each joint to the displacement of the fingers is derived from the angular displacement of that particular joint, a sequel to the force applied to the member or the moment it generates. The total linear distance travelled either is calculated from the total angular distance or plotted in CAD design and measured. Due to the length and complexity of these equations which are given in [14], most of the calculations were done using MATLAB software.

The active elements are inclined 46.08° to the transverse axis.

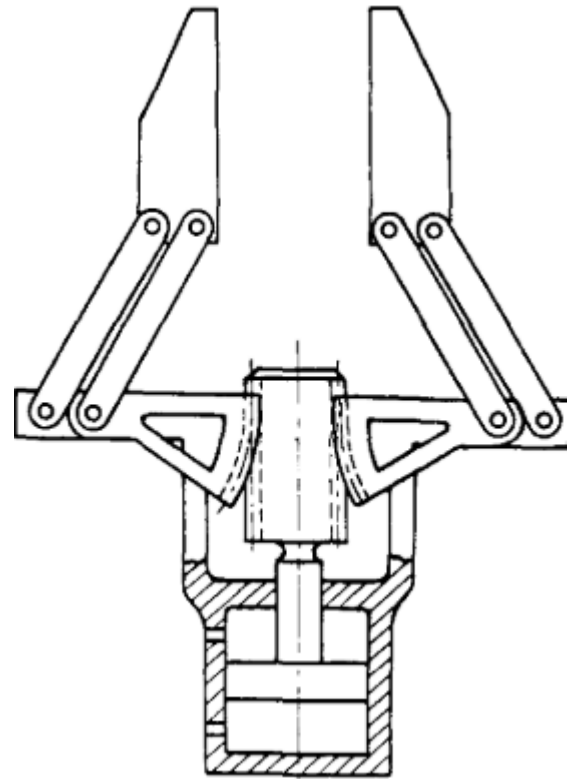


Fig. 3. Rigid jointed gripper with element linkage similar to the proposed gripper design[24]

TABLE II
JOINT DISTANCE FROM ACTIVE ELEMENTS AND CORRESPONDING MOMENTS

| Joint Number | Distance from My_1 | Distance from My_2 | Moment My_1 | Moment My_2 |
|--------------|----------------------|----------------------|---------------|---------------|
| 1 | 0.00182 | 0.01718 | 0.0084 | 0.0794 |
| 2 | 0.01682 | 0.03218 | 0.0777 | 0.1487 |
| 3 | 0.03182 | 0.04718 | 0.1471 | 0.2181 |
| 4 | 0.04682 | 0.06218 | 0.2164 | 0.2874 |
| 5 | 0.06182 | 0.07718 | 0.2857 | 0.3567 |
| 6 | 0.07682 | 0.09218 | 0.3551 | 0.4261 |
| 7 | 0.09182 | 0.10718 | 0.4244 | 0.4954 |
| 8 | 0.10682 | 0.02004 | 0.4937 | 0.0926 |
| 9 | 0.01860 | - | 0.0860 | - |

This gives a tension T of 4.165 N in each element after resolving the forces at the acting point. The two parallel links experience the same force.

The moment about the flexure hinge at the base will vary for different flexure joints. The distance of each joint from the active elements is summarized in Table 2. The moment due to the force applied differs for each joint. Moment My_1 is for the outer link and moment My_2 is for the inner link. The moments are also tabulated in Table 2. Since the gripper has geometric symmetry, only one side of the gripper is considered for analysis. Joint displacement summary is given in Table 3.

The angular displacement is in degrees and has to be converted to radians.

$$Linear\ displacement = r\theta_1 + r\theta_2 \quad (11)$$

where r is 106.3mm

As expected, the lowest flexure joints at the base area expe-

TABLE III
ANGULAR DISPLACEMENT CONTRIBUTION FOR EACH JOINT

| Joint Number | Angular Displacement ₁ | Angular Displacement ₂ |
|--------------|-----------------------------------|-----------------------------------|
| 1 | 0.0036 | 0.0342 |
| 2 | 0.0335 | 0.0640 |
| 3 | 0.0633 | 0.0938 |
| 4 | 0.0931 | 0.1237 |
| 5 | 0.1230 | 0.1535 |
| 6 | 0.1528 | 0.1833 |
| 7 | 0.1826 | 0.2132 |
| 8 | 0.2125 | 0.0399 |
| 9 | 0.0370 | - |

rience more displacement than the ones above them. Furthermore, the displacement, though unequally shared, is distributed across all the joints, which satisfies the design requirements. The inner links of the parallelogram setup evidently experience a slightly higher deformation than the outer links because they are directly linked to the applied force. When the angular displacement is resolved from CAD design, it amounts to 3.96mm. The various results are depicted in Fig 4 for comparison.

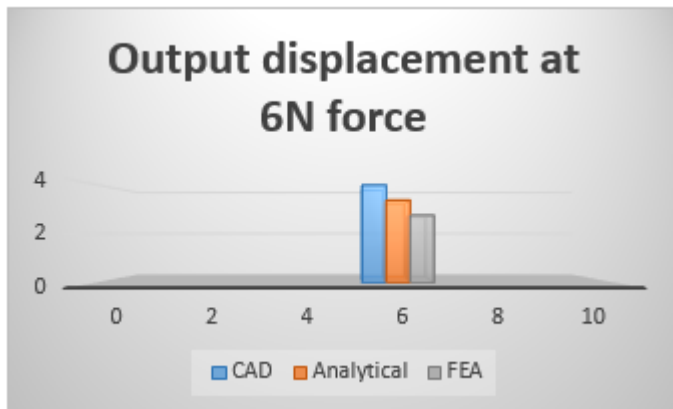


Fig. 4. Graph of comparison between CAD, FEA and analytical output displacement results at 6N force

IV. DESIGN PROTOTYPE AND DEVELOPMENT

A. MODEL

After the implementation of the design criteria, dimensions and various orientations were realized. A 3D model was designed, as shown in Fig 5.

B. FABRICATION

Subtractive manufacturing using laser machining was employed. 3mm thickness Plexiglas was used. The fabricated prototype is shown in Fig 6. The actuator and the actuating point have been installed and fastened successfully.

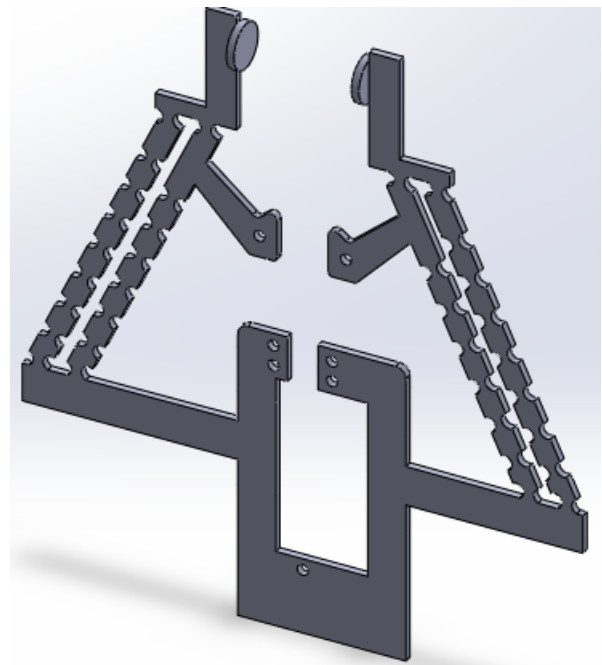


Fig. 5. Modelled gripper with flexure joints for macroscale grasping

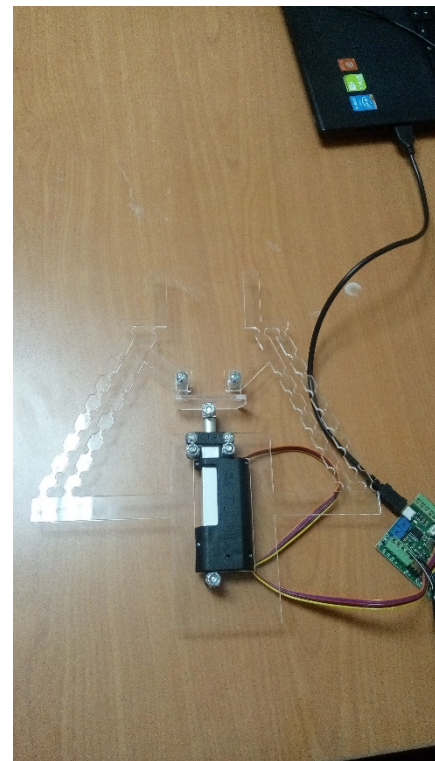


Fig. 6. Fabricated gripper prototype with installed actuator

C. SIMULATION

The allowable stress for the gripper elements is 46MPa. However, the stress values experienced in the gripper are kept further away from this nominal value so as to increase the number of cycles the gripper can make in its lifetime. If structural fatigue was not taken into consideration, the gripper could obtain a displacement of 18mm.

The 3D safe stress profile is given in Fig 7. The colour bar beside the structure indicates the extremities of stress concentration, with the maximum stress regions being indicated by red colour, and the least stressed regions are in blue colour. The maximum stress regions lie at the top flexure joints. This is because in the parallelogram setup, those are the joints responsible for maintaining the translational motion of the gripper throughout the deformation process. After grasping, the uppermost joints will experience reaction forces as well. Hence, in the event of failure, the gripper is likely to fracture in those areas. The lower joints also experience greater stress, and the stress deteriorates as one ascends up the links until it reaches its lowest joint stress at the flexure joint closest to the active elements.

The 3D safe displacement profile is given in Fig 8. The colour bar beside the gripper is a deformation indicator, with the maximum deformation being indicated by red colour, and the least deformation being shown blue colour. As desired, the maximum deformation is experienced by the gripper fingers.

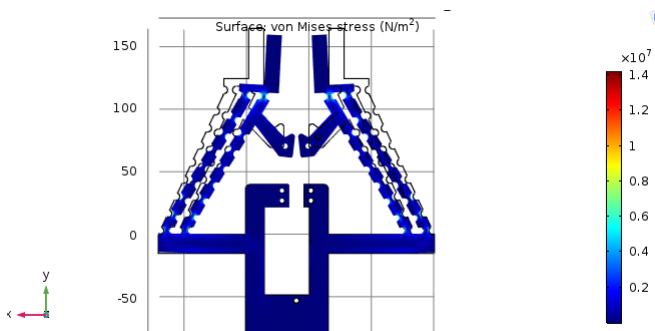


Fig. 7. Simulation results for stress analysis

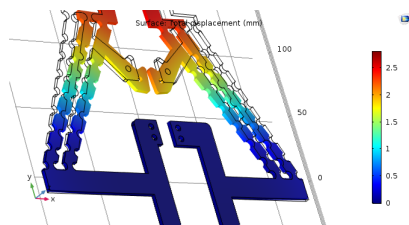


Fig. 8. Simulation results showing displacement distribution within the gripper

The plot for simulated data for input force against output displacement is given in Fig 9. This shows how the displacement of the gripper progresses with each step increment in force until the 6N force is reached. The graph is linear, which implies that there is a proportional increment in displacement with gradual force increment, and vice versa. However, for larger forces (above 10N), linearity is lost, which makes the force control of flexure-based gripper demanding in such circumstances.

V. OTHER RECOMMENDATIONS

The developed prototype can be used to conduct experiments on kiwifruit in order to verify whether the gripper

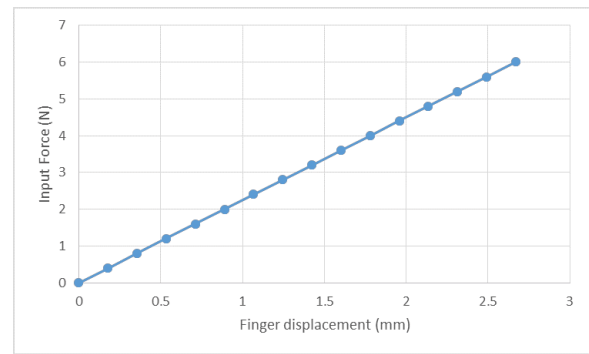


Fig. 9. Force-displacement correlation graph

can indeed achieve the expected displacements and withstand the forces involved. Feedback control can be established on the gripping system and hence make the gripper smart. This would better maintain the quality of the fruits even after the gripping and manipulation process has been accomplished. Fatigue analysis has to be carried out to reveal the number of cycles the gripper can perform. A thorough optimization process has to be adopted and applied to the links so as to optimize the number of flexure joints

VI. CONCLUSION

The analytical design of the gripper reveal how applicable the model can be at macroscale. The total displacement achievable in the fingers is greater than 6mm, which is sufficient to conduct successful conventional grasping operations. The stress factor of the gripper is kept below half the allowable stress of the gripper structure material. The simulation results were closely approaching the analytical results. It can be seen, however, in the simulation results that a slight deflection the y-direction occurs. The magnitude of this displacement at the finger area is less than 1 mm (the maximum is 0.9mm). Therefore at macroscale, this displacement is small enough to cause any significant rotational movement during grasping hence, negligible.

ACKNOWLEDGEMENT

N. N. Mrewa would like to thank Pan African University for the opportunity to study at the institution and provide for me platform for higher education. N. N. Mrewa would also like to show appreciation to E-Just for allowing the author to conduct experiments and other research procedures at their institution. They opened up their staff and the resources for the purposes of this research.

REFERENCES

- [1] A. A. Escriva, Design of a Smart Gripper for Industrial Applications, Tampere University of technology, 2016.
- [2] T. Bock, J. Herbst, C. Balaguer, and M. Abderrahim, Design of a Gripping System for the Automated Assembly of Large Building Modules, Proc. 17th IAARC/CIB/IEEE/IFAC/IFR Int. Symp. Autom. Robot.

Constr., 2017.

[3] S. A. Journal and I. E. May, Testing Flexible Grippers for Geometric and Surface Grasping Conformity in, vol. 29, no. May, pp. 128142, 2018.

[4] Y. Tsai, S. H. Lei, and H. Sudin, Design and analysis of planar compliant microgripper based on kinematic approach, J. MICROMECHANICS MICROENGINEERING, no. October 2004, pp. 143156, 2005.

[5] A. Nikoobin and H. M. Niaki, Deriving and analyzing the effective parameters in microgrippers performance, Sci. Iran. B, vol. 19, no. 6, pp. 15541563, 2012.

[6] S. K. Nah and Z. W. Zhong, A microgripper using piezoelectric actuation for micro-object manipulation, Sensors Actuators, A Phys., vol. 133, no. 1, pp. 218224, 2007.

[7] L. L. Howell, Compliant mechanisms. Wiley, 2001.

[8] J. A. Gallego and J. Herder, Synthesis Methods in Compliant Mechanisms: An Overview, pp. 193214, 2010.

[9] S. Krishnan and L. Saggere, Design and development of a novel micro-clasp gripper for micromanipulation of complex-shaped objects, Sensors Actuators, A Phys., vol. 176, pp. 110123, 2012.

[10] I. Q. Meng, Meccanica e Scienze Avanzate dell Ingegneria A Design Method for Flexure-Based Compliant Mechanisms on the Basis of Stiffness and Stress Characteristics, pp. 1110, 2012.

[11] H. E. Stephanou and G. D. Skidmore, Imece2003- 55013 imece2003-44013, 2016.

[12] O. F. Linkage-type, Mech. Mach. Theory, no. 97, 1997.

[13] M. Verotti, A. Dochshanov, and N. P. Belfiore, A Comprehensive Survey on Microgrippers Design: Mechanical Structure, J. Mech. Des., vol. 139, no. 6, p. 060801, 2017.

[14] F. Dirksen, Non-intuitive Design of Compliant Mechanisms Possessing Optimized Flexure Hinges, p. 240, 2013. [15] Physical Properties of Acrylic Sheets.

[16] G. Causey, Guidelines for the design of robotic gripping systems, Assem. Autom., vol. 23, no. 1, pp. 1828, 2003.

[17] Y. Liu and Q. Xu, Design and analysis of a micro-gripper with constant force mechanism, Proc. World Congr. Intell. Control Autom., vol. 2016September, pp. 21422147, 2016.

[18] W. Ai and Q. Xu, New structural design of a compliant gripper based on the Scott-Russell mechanism, Int. J. Adv. Robot. Syst., vol. 11, 2014.

[19] Y. Liu and Q. Xu, Mechanical design, analysis and testing of a large-range compliant microgripper, Mech. Sci., vol. 7, no. 1, pp. 119126, 2016.

[20] G. Hao and R. B. Hand, Design and static testing of a compact distributed-compliance gripper based on flexure motion, Arch. Civ. Mech. Eng., vol. 16, no. 4, pp. 708716, 2016.

[21] D. Of and S. U. Compliant, DETC2006-99415, pp. 19, 2017.

[22] M. Liu, X. Zhang, and S. Fatikow, Design of flexure hinges based on stress-constrained topology optimization, J. Mech. Eng. Sci., vol. 0, no. 0, pp. 111, 2016.

[23] Miniature Linear Motion Series Datasheet, 2016.

[24] F. Y. Chen, Force Analysis and Design Considerations of Grippers., Ind. Rob., vol. 9, no. 4, pp. 243249, 1982.

[25] D. Kern, M. Rsner, E. Bauma, W. Seemann, R.

Lammering, and T. Schuster, Key features of flexure hinges used as rotational joints: Transition from concentrated to distributed compliances, Forsch. im Ingenieurwesen/Engineering Res., vol. 77, no. 34, pp. 117125, 2013.

[26] Standards for seeds, tractors, forest, fruit and vegetables - OECD. [Online]. Available: <http://www.oecd.org/tad/code/>. [Accessed: 16-Feb-2019].